

Capture, Storage and Use of CO₂ (CCUS)

Dynamic storage capacity evaluation for the Hanstholm and
Havnsø structures

Carsten M. Nielsen

Capture, Storage and Use of CO₂ (CCUS)

Dynamic storage capacity evaluation for the Hanstholm and
Havnsø structures

Carsten M. Nielsen

Dynamic storage capacity estimation for the Hanstholm and Havnsø structures

Carsten M. Nielsen

Preface

Late 2019, GEUS was asked to lead research initiatives in 2020 related to technical barriers for Carbon Capture, Storage and Usage (CCUS) in Denmark and to contribute to establishment of a technical basis for opportunities for CCUS in Denmark. The task encompasses (1) the technical potential for the development of cost-effective CO₂ capture technologies, (2) the potentials for both temporary and permanent storage of CO₂ in the Danish subsurface, (3) mapping of transport options between point sources and usage locations or storage sites, and (4) the CO₂ usage potentials, including business case for converting CO₂ to synthetic fuel production (PtX). The overall aim of the research is to contribute to the establishment of a Danish CCUS research centre and the basis for 1-2 large-scale demonstration plants in Denmark.

The present report forms part of Work package WP6 and focuses on the use of reservoir (flow) simulation methodologies to estimate storage capacities for the Havnsø and Hanstholm structures.

Content

Dansk Sammendrag	3
Summary	4
Introduction	5
Reservoir simulation methodology	6
Reservoir Properties.....	6
Saturation functions.....	8
PVT Data.....	9
Simulation boundary conditions	10
Simulation initialization	10
Reservoir simulation models, Havnsø and Hanstholm	11
CO ₂ Injection.....	12
Simulation results and discussion	13
Conclusion	19
Recommendations for future work	20
References	21

Dansk Sammendrag

Reservoirsimuleringer udført for Havnsø strukturen indikerer, at strukturen kan indeholde mere end 250 Mt CO₂, og at 3 Mt CO₂ årligt kan pumpes ind i strukturen med en gennemsnitlig pumperate på 1 Mt CO₂/år/brønd fordelt ligeligt på 3 injektionsbrønde. Dette indebærer et estimeret overtryk i Gassum Formationen på maksimalt 240 bar inden for en periode på 90 år, det vil tage at fylde strukturen med CO₂. Overtrykket i Gassum Formationen kan holdes under det kritiske fraktureringstryk for formationen, som er sat til 75% af det lithostatisketryk. Det kritisk kapillære tærskeltryk, der indebærer en risiko for at CO₂ bryder gennem Fjerritslev Formationens lagserie af muddersten, anslås til at være minimum 60 bar. Med et relief på strukturen på ca. max 300 m, vil en CO₂ kolonne på 300 m maksimalt udøve et kapillartryk på ca. 13 bar mod seglet, hvilket er ca. 4 gange lavere end Fjerritslev Formationens kapillære tærskeltryk.

For Hanstholm strukturen indikerer simuleringer, at strukturen kan indeholde op til 1000+ Mt CO₂, og at 8 Mt CO₂ årligt kan pumpes ind i strukturen med en gennemsnitlig pumperate på 1 Mt CO₂/år/brønd fordelt ligeligt på 8 injektionsbrønde. Dette indebærer et estimeret overtryk i Gassum Formationen på maksimalt 220 bar inden for en periode på 125 år, som det vil tage at fylde strukturen med CO₂. Som for Havnsø vil trykket i selve reservoiret ikke overstige det kritisk overtryk, der indebærer frakturering af formationen. Relieffet på Hanstholm Strukturen er op til ca. 500 m, hvilket kan give et kapillartryk på ca. 22 bar, hvilket igen er betryggeligt under et kapillærtærskel tryk på de 60 bar for den forseglende bjergart.

Tilsammen har de to strukturer således en lageringskapacitet på ca. 1600+ Mt CO₂, svarende til mere end 100 års CO₂-udledning fra de største Danske CO₂-udledere med en samlet udledning på 5-9 Mt CO₂/år. Ovennævnte estimer er dog baseret på "version_0" reservoirmodeller, som kun i begrænset omfang bygger på de mange geologiske data, der er opnået i CCUS projektet.

Summary

Reservoir simulations performed for the Havnsø structure indicate that the structure can contain more than 250 Mt CO₂, and that 3 Mt CO₂ can be pumped into the structure annually with an average pumping rate of 1 Mt CO₂ / year / well evenly distributed over 3 injection wells. This gives an estimated overpressure in the Gassum Formation of maximum 240 bar within the period of 90 years, it will take to fill the structure with CO₂. The overpressure in the Gassum Formation can be kept below the critical fracture pressure for the formation, which is set at 75% of the lithostatic pressure. The critical capillary threshold pressure, which causes a risk of CO₂ breaking through the Fjerritslev Formation is estimated to be a minimum of 60 bar. With a relief on the structure of approx. max 300 m, a CO₂ column of 300 m will exert a maximum capillary pressure of approx. 13 bar against the seal, which is approx. 4 times lower than the capillary threshold pressure of the Fjerritslev Formation.

For the Hanstholm structure, simulations indicate that the structure can contain up to 1000+ Mt CO₂, and that 8 Mt CO₂ can be pumped into the structure annually with an average pumping rate of 1 Mt CO₂ / year / well evenly distributed over 8 injection wells. This implies an estimated overpressure in the Gassum Formation of maximum 220 bar in a period of 125 years, which will take to fill the structure with CO₂. As for the Havnsø structure, the pressure in the reservoir will not exceed the critical overpressure that can fracture the formation. The relief on the Hanstholm structure is up to approx. 500 m, which can give a capillary pressure of approx. 22 bar, which is safe below a capillary threshold pressure of 60 bar for the cap rock.

Together the two structures have a storage capacity of approx. 1600+ Mt CO₂, corresponding to more than 100 years of CO₂ emissions from the largest Danish CO₂ emitters with a total emission of 5-9 Mt CO₂ / year. However, the above estimates are based on "version_0" reservoir models, which are only to a limited extent based on new and re-interpreted geological data obtained in the CCUS project.

Introduction

One of the objectives in the CCUS project is to evaluate the CO₂ storage potential for two selected structures, *i.e.* the Havnsø structure located Northeast of Kalundborg and below the small village Havnsø and the Hanstholm structure approximately 25 km offshore to the Northwest of Hanstholm Port. For both structures the Gassum Sandstone Formation forms the storage reservoir and the overlying Fjerritslev Formation containing thick layers of shales forms the sealing layer. Both structures are at present interpreted to be in the form of 4-way dip domal closures.

Storage capacity for subsurface geological storage of CO₂ can be estimated by two different methodologies; a static capacity estimation calculation and a dynamic capacity simulation. The fundamental difference between the two methods is the way the CO₂ is filled into the reservoir. In the static calculation the CO₂ is modelled to fill all available pore space above a certain threshold (*e.g.* spill point and N/G). To mimic a practical application, where the CO₂ phase will not effectively find its way to all available pore spaces a filling efficiency factor are used. For the dynamic capacity estimation reservoir simulation methodologies are used to simulate a realistic CO₂ injection process, where the CO₂ phase spreads into the reservoir from predefined injection points. The dynamic capacity estimation thereby depends on internal reservoir continuity and the choice of operational conditions for a specific injection process, *i.e.* the number of wells, well locations, injection rate and cumulate injection time.

For both methodologies an essential step is to determine a geological understanding or model of the individual structures to be evaluated. For the static capacity estimation distributions in reservoir properties such as porosity, N/G, reservoir thickness and areal delineation are decisive for the calculated results. Uncertainties in the resulting estimations can be assessed by applying probability distributions in the individual properties going into the calculations (Hjelm *et al.*, 2020). For a dynamic calculation of storage capacity, the geological model (reservoir model) must also account for flow and migrations pathways in the reservoir together with the above-mentioned operational constraints. Thereby a scenario approach to evaluate and determine uncertainties in the dynamic storage capacity calculations is useful.

The present report describes a series of reservoir simulations undertaken to assess the (dynamic) CO₂ storage capacity for the Havnsø and Hanstholm structures. Construction of the reservoir (static) models for the two structures are described in Frykman (2020a and 2020b). The Petrel software was used to construct the reservoir models (Petrel 2017), whereas the reservoir simulation software Eclipse 100 (Eclipse 2017) was used to perform the simulations, both software's are licensed by Schlumberger.

Reservoir simulation methodology

The dynamic modelling of injection of CO₂ into the structures for permanent storage is performed using the oil & gas industry standard reservoir simulator Eclipse (Eclipse, 2017). The simulator is a fully implicit, three phase and three-dimensional general purpose black oil simulator. The “black oil” term references to the way oil is modelled in the simulator; oil is treated as one lumped component *i.e.* no variation in the oil composition other than dissolved gas.

Only the oil and gas phases are used in the present simulations. To mimic the process of injecting CO₂ into an aquifer the simulator oil phase is given PVT and phase data corresponding to the formation brine and the simulator gas phase is assigned properties corresponding to CO₂. PVT, solubility data and viscosities are represented by tables in the simulator input files. This allows both solubility properties and density versus depth data to be consistently represented, as pressure variation in the model is dominated by the hydrostatic pressure gradient in the initialization of the simulations. During simulations of the injection process the pressure development in the reservoir will be governed by the choice of well configuration, injection rate(s) and the distribution of reservoir properties, especially the distribution of permeabilities and the distribution of sand and shale.

The phase behaviour is described by black-oil PVT tables and CO₂ densities for the PVT table are calculated by the Soave-Redlich-Kwong equation-of-state as modified by Peneloux (Peneloux *et al.* 1982).

The governing flow equations used to model the CO₂ injection process are Darcy’s equation and conservation of mass. The differential equations are solved by numerical techniques on a modelling grid. Eclipse 100 (Eclipse, 2017) uses the finite difference technique. The modelling grid is constructed in the Petrel software (Petrel, 2017), where all the geological information and interpretations are built into a reservoir (static) 3D model. Two static models are in use to assess dynamic storage capacities for the Havnsø and Hanstholm structures, respectively (Frykman, 2020a, 2020b). To assess uncertainties and geological variability in the reservoir models four different scenarios for the Havnsø model were used for the reservoir simulation work.

As stated previously in the CCUS project the reservoir models are labelled version_0 models, this means that the models are built mainly on existing data and interpretations. Next step is to include all new acquired/processed data and geological, geophysical and petrophysical interpretations.

Reservoir Properties

Grids with properties for the Havnsø and Hanstholm reservoir models were exported from the Petrel software to be used in the Eclipse 100 reservoir simulator (Frykman, 2020a, 2020b). The simulation grids are corner point grids, *i.e.* Cartesian grids, where the individual grid cells can be skewed to encompass different geological features.

The Reservoir properties exported were the porosity and facies distributions. Permeabilities were calculated from porosity permeability relation(s), figure 1.

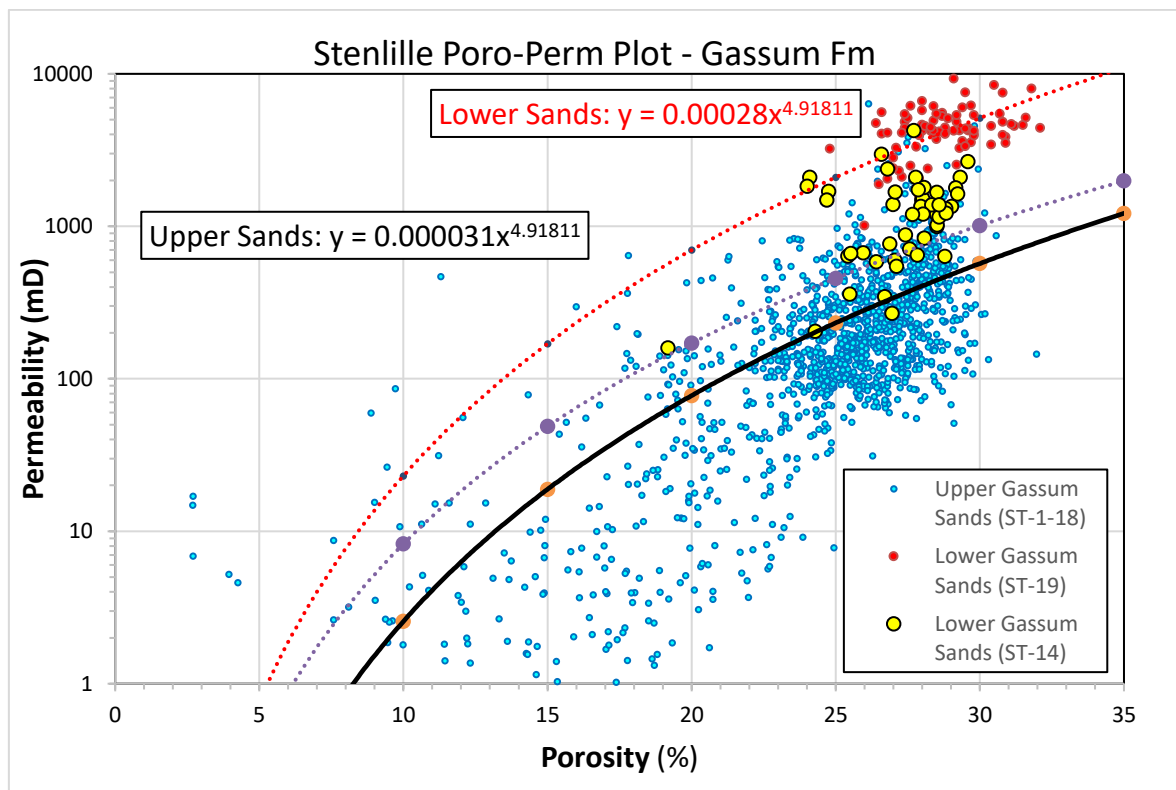


Figure 1: Porosity-permeability relationships for the Gassum Formation sandstones. Based on conventional core analysis data from cored Stenlille wells. The black line represents the upper part of the Gassum Formation, the red line represents the lower part of the Gassum Formation. Permeability values are gas permeabilities measured on core plugs. (Kristensen, 2020).

Two different permeability models are shown in figure 1 with trend lines labelled “Upper Sands” and Lower Sands”. The “Upper Sand” model was used in most of the simulation runs, whereas the “Lower Sands” model was used to show a potential upside in the modelling. The measured permeabilities in figure 1 are gas permeabilities, a factor of 0.5 was multiplied on the permeability values to convert to fluid permeability.

The permeability model(s) were used only for the sands, the shale layers were assigned a constant permeability of 0.01 mD for the shale layers interbedded in the reservoir section and a value of 0.001 mD was used for the cap rock, assessed from Springer *et al.*, 2020. The ratio of vertical to horizontal permeability was set to 0.3, both for the sands and shales. Sensitivity on the ratio, ranging from 0.2 to 0.5 showed no influence on the simulation results, as it is the capillary entry pressure that controls most of the vertical and buoyant flow.

Saturation functions

Due to the two-phase fluid system, when injecting supercritical CO₂ into a water filled reservoir, relative permeabilities must be applied to model the effect on permeability reduction, when more than one phase is present in the pore space. Two sets of relative permeability functions were used to model the effect on the storage capacity (Bennion & Bachu, 2006(1), Berg & Ott, 2012), *cf.*, figure 2. For simplicity and simulation run time optimization hysteresis was only modelled for the non-wetting phase *i.e.* the CO₂ phase. This means that the relative permeabilities are different when the CO₂ saturation is increased in a grid cell during the filling process and when CO₂ is leaving a grid cell. This effect will be present, when CO₂ is injected down flank of the structure; first the CO₂ saturation will increase around the injection point but due to buoyancy the CO₂ will migrate to the top of the structure resulting in a long tail of residual trapped CO₂. The Killough scanning method was applied in the Eclipse simulations (Eclipse 100, 2017). The method governs how the reversal in saturation increase/decrease is modelled from the bounding relative permeability functions. The permeability functions were used both for the reservoir sands and the interbedded shale layers.

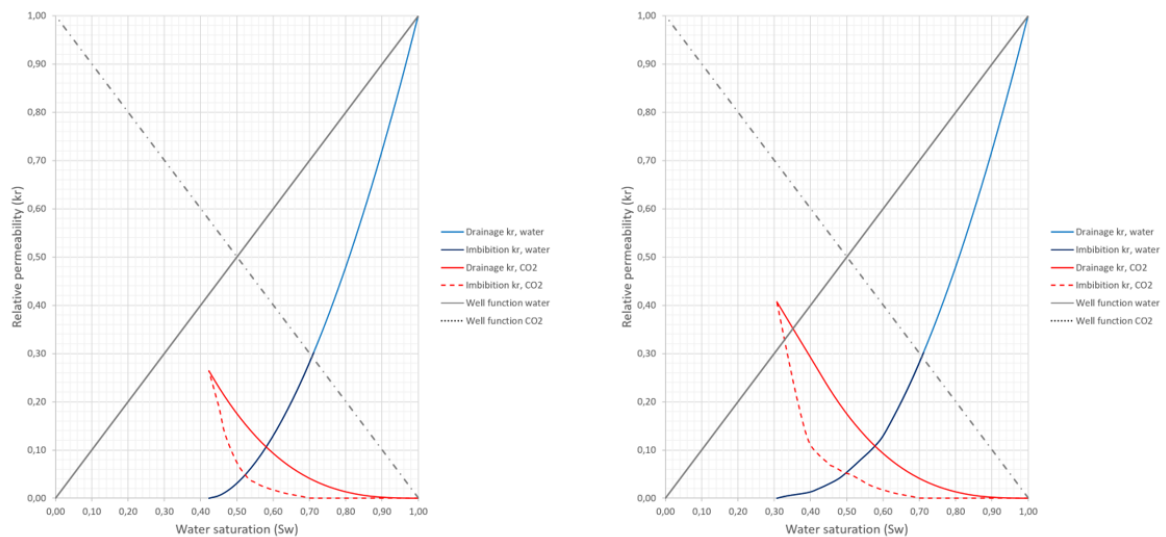


Figure 2. Relative permeability functions. Left: modified from Bennion & Bachu (2006(1)), only hysteresis in the non-wetting phase. Residual water saturation is 0.42. Right: Curves modified to have residual water saturation of 0.30 (modified from Berg & Ott (2012)). For the well/reservoir flow straight lines with no residual saturations were used.

In two phase flow in porous rocks capillary pressure forces are present and is modelled by capillary pressure functions, figure 3. As for the relative permeabilities hysteresis are present and two sets of bounding curves are used. Again, the Killough scanning method was applied (Eclipse 100, 2017).

In figure 3 is only shown the capillary pressure functions for the reservoir sands. The capillary entry pressure is set to 0.1 bar, *i.e.* the minimum over-pressure in the CO₂ phase needed to start forcing CO₂ in the porous rock. The 0.1 bar capillary entry pressure is of the same

magnitude given in Bennion & Bachu (2006(2)). For the shale layers the capillary pressure values is multiplied by a factor of 100, resulting in a capillary entry of 10 bar. For the sealing rock a value of 200 was used, resulting in an entry pressure of 20 bar, which is sufficient to withstand a high CO₂ column of more than 400 m. It is a conservative value, Springer *et al.*, (2020), find higher shale entry pressures.

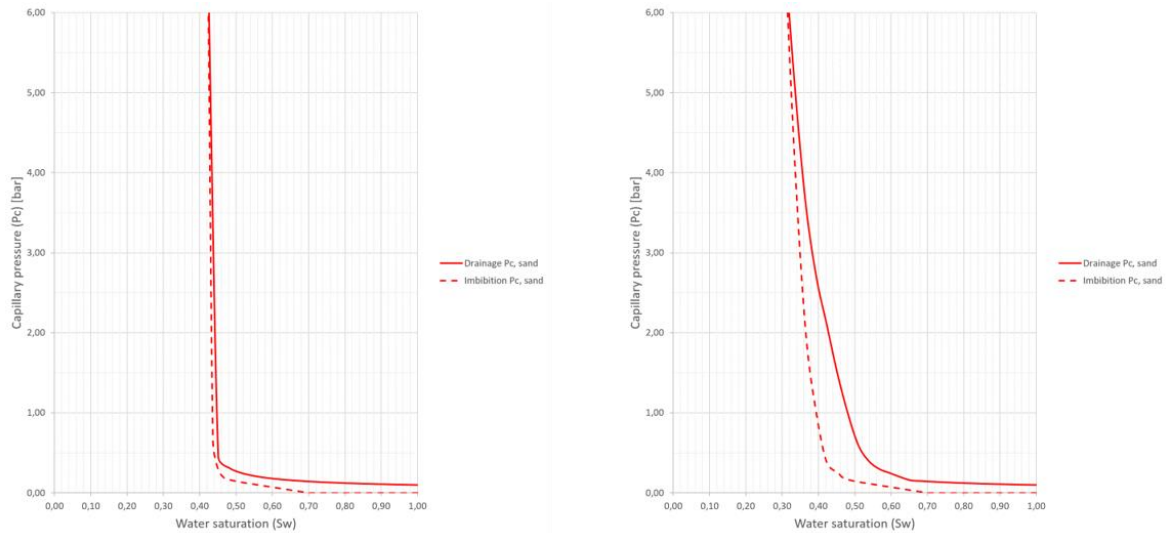


Figure 3. Capillary pressure functions for sand, drainage and imbibition. Left: residual water saturation of 0.42 to mirror residual water saturation in relative permeabilities (Bennion & Bachu (2006)). Right: Curves modified to have residual water saturation of 0.30.

PVT Data

As stated above the simulator oil phase is given PVT and phase data corresponding to the formation brine and the simulator gas phase is assigned properties corresponding to CO₂.

Depth gradients for pressure and temperature are assessed to be at equilibrium at initialization of the simulations. At standard conditions ($T = 10^{\circ}\text{C}$, $P = 1$ bar) the formation water density is assigned a value of 1100 kg/m^3 for both the Havnsø and Hanstholm models. A temperature gradient of $28^{\circ}\text{C}/1000\text{m}$ with an average surface temperature of 8°C is used for both models.

The CO₂ formation volume factor (FVF), density and viscosity are obtained from the commercial PVT software PVTsim_v11.5 (Calsep 2001). The water data which accounts for dissolved CO₂ are obtained from Chang, Coats and Nolen (1998).

The brine density as function of pressure is calculated by the correlation of Rowe and Chow (1970). The brine viscosity is assumed to be independent of CO₂ content and pressure. It is calculated by the correlation of Batzle and Wang (1982).

CO₂-in-water diffusion is not included in the present set-up as the effect is negligible with a time scale of 100 years. If, however the long-term behaviour and fate of the sequestered CO₂ is to be assessed, the diffusion of the CO₂ in the water phase can be implemented in Eclipse 100.

Simulation boundary conditions

To ensure that the model boundaries don't influence the modelling results the "pore volume multiplication" method is used as a boundary condition. The pore volumes of the outermost grid cells of the model have been multiplied by a high number to mimic that the model area is situated in an almost infinite aquifer. In Eclipse this is controlled by the MULTPV key word. For the present simulations a factor of 1000 was used.

The constraints set on the wells in the simulator also act as boundary conditions. The Eclipse 100 "well option" is used to secure the flow performance between the wellbore and the reservoir is modelled as realistic as possible. The well option uses an analytical solution for the pressure build-up in the near wellbore area (grid cells). Wells are setup as vertical wells with a well diameter of 0.25 m. All wells are completed in the lower part of the reservoir intervals for the Havnsø and Hanstholm models, respectively. A skin factor (flow resistance in the near well area) of 0 is used; *i.e.* no extra resistance for flow to the reservoir from the wellbore. The wells are operated with a constant injection rate set to 1 Mt pr. year pr. well and controlled with a maximum limit on the bottom hole pressure not exceeding the formation fracture pressure. For both the sand and shale layers the formation fracture pressure was set to 75% of the lithostatic pressure. This limit needs further investigation, but 75% is assessed to be a conservative estimate.

Simulation initialization

The simulation runs are initialized from hydrostatic conditions and with the above temperature gradient. It is assumed that the reservoirs are in hydraulic and thermal equilibrium. The initial datum pressure is calculated from the depth and formation water density.

The wells are operated at maximum load at the start of simulations, *i.e.* no attempt to ramp up the injection pressure for safety reasons.

Reservoir simulation models, Havnsø and Hanstholm

The two static models for the Havnsø and Hanstholm structures (Frykman, 2020a, 2020b) were populated with reservoir properties in the Petrel software as described above. Grids with properties were exported to the Eclipse 100 format for subsequent reservoir simulation. Grids and initial conditions are shown in table 1. The 3D models with injection well locations are displayed in figure 4.

Reservoir	Grid		Initial conditions			Injection
	nx, ny, nz	dx, dy, dz [m]	Datum [m]	T [°C]	P @ Datum [bar]	Rate [tonnes/y]
Havnsø	160, 200, 155	100, 100, 1 (av.)	1200	42	130	1E6
Hanstholm	86, 104, 52	400, 400, 2 (av.)	1000	36	108	1E6

Table 1.

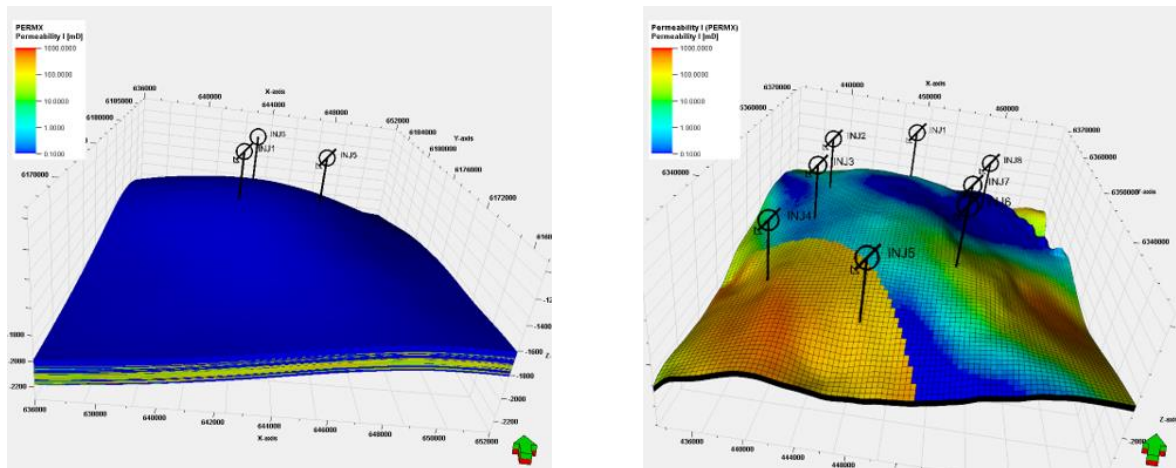


Figure 4. Left: Havnsø model covering an area of 16 km x 20 km. Figure displays the permeability distribution, the top layers are the caprock with a constant and low permeability. 3 injection wells. Right: Hanstholm model covering an area of 34 km x 42 km. The caprock is stripped off showing the permeability distribution on the top reservoir layer. 8 injection wells.

To reflect uncertainties in the interpreted depositional environment four depositional model scenarios were constructed for the Havnsø structure. The orientation of the depositional direction and different net-to-gross ratio for sand/shale layers were varied, cf. Figure 5A and 5B (Frykman, 2020b). The absolute permeability was varied for some of the models with permeability factors of 0.5 and 2. Further the relative permeability was varied by shifting the residual water saturation from 0.42 to 0.30 as shown in figure 2 and 3. Finally the number of injection wells used to fill the structure was varied from 3 to 5

For the Hanstholm structure only a single model was constructed and used for reservoir simulation. A total number of 8 wells were used to fill the structure.

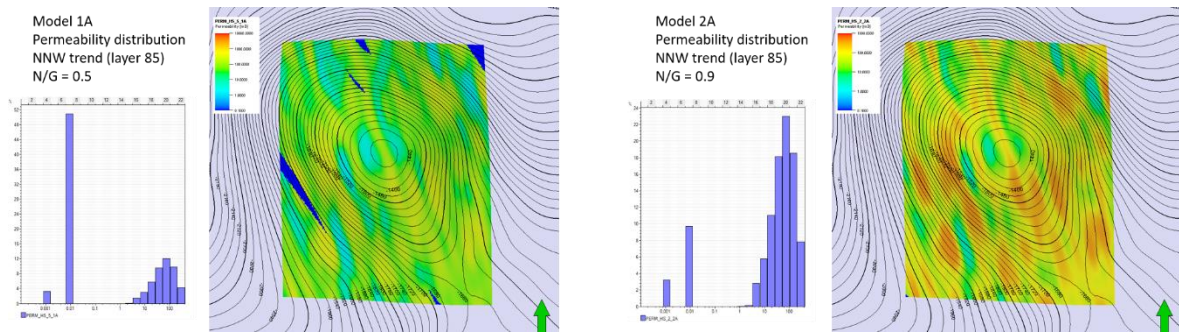


Figure 5A. Havnsø model with NNW trend on sand/shale layers. Left: N/G 0.5. Right: N/G 0.9.

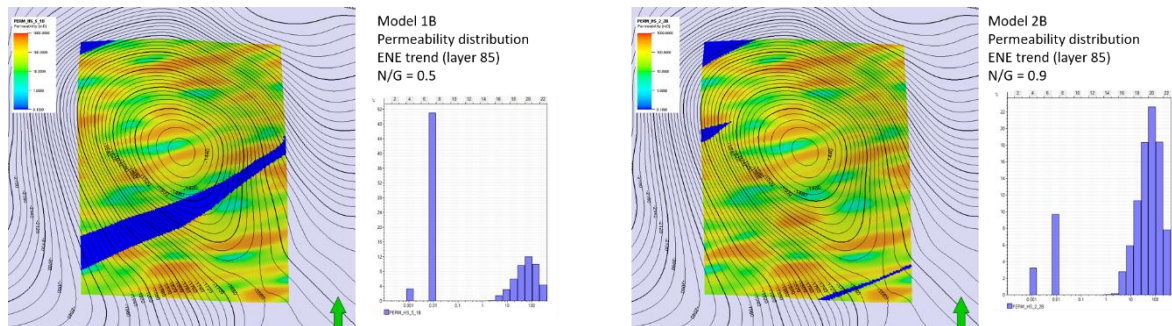


Figure 5B. Havnsø model with ENE trend on sand/shale layers. Left: N/G 0.5. Right: N/G 0.9.

CO₂ Injection

All simulations were run with a constant CO₂ injection rate of 1 Mt/year and all wells were controlled by rate and a limit on the flowing bottom hole. The injection rate was selected with reference to the Sleipner CCS project, where CO₂ injection in a single well at a rate of 900.000 to 1 Mt/year has been operated since 1996. It is assumed that a similar single well rate can be achieved in a potential future storage operation at the two structures.

All simulations were initialized from hydrostatic conditions as described previously.

For both the Havnsø and Hanstholm models a series of simulation cases were run to optimize the well location on the individual structures. This was done by trial & error with the constraints that CO₂ do not spill out of the structural closures and the field pressure is kept below the fracture threshold pressure. The fracture threshold pressure was limited to 75% of the lithostatic pressure.

The Havnsø model with the ENE depositional trend and a N/G of 0.5 was used as a base case for comparison of different simulation scenarios (*cf.* figure 5B, left). The base case simulation was optimized to fill the structure as much as possible with CO₂ under the above constraints. The other simulation cases were run with identical well location and injection time.

Simulation results and discussion

Simulation results are presented as pressure versus depth diagrams, where the simulated field pressure for each simulation grid cell is plotted. A diagram showing the resulting CO₂ distribution relative to the top reservoir surface is also presented to verify that the CO₂ plume is securely contained within the closure of the structure.

Figure 6 shows the result for the base case; three injection wells operated at a constant injection rate of 1 Mt/year.

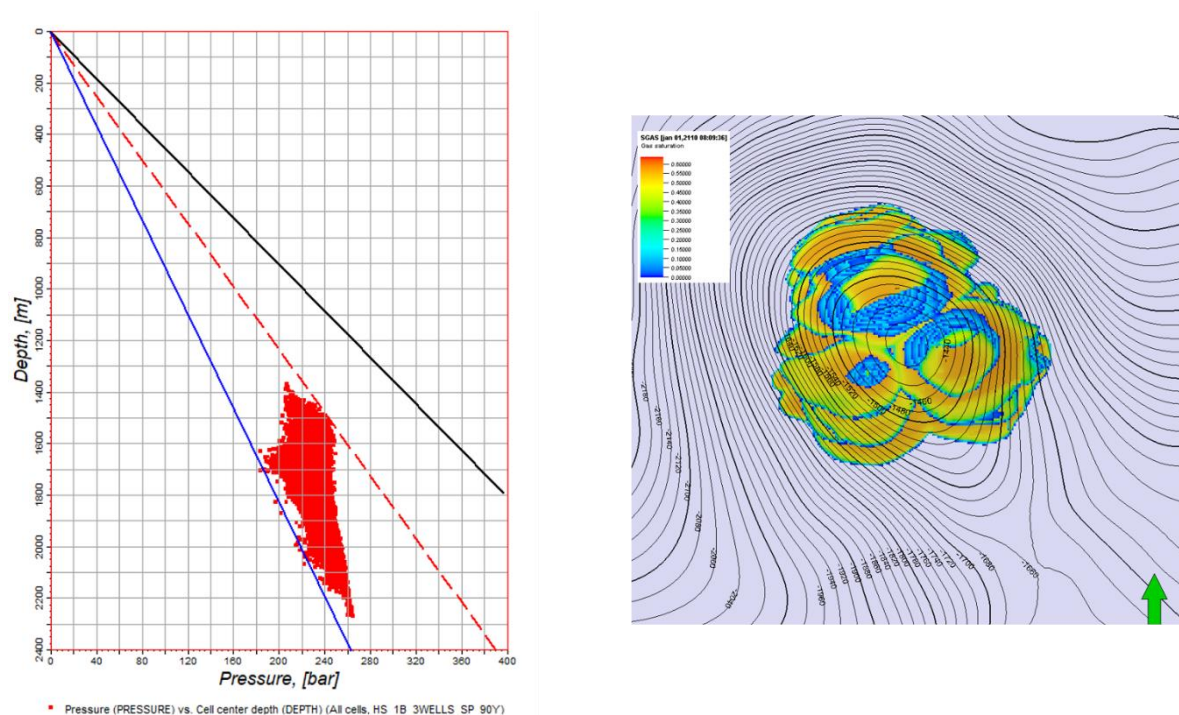


Figure 6. Left: Pressure versus depth diagram, blue line is the hydrostatic pressure, black line is the lithostatic pressure, red dotted line is the fracture threshold of 75% of the lithostatic pressure, red squares are the simulated grid cell pressure. Right: CO₂ distribution within the structural closure.

The simulation was run for 90 years resulting in a total injection of 270 Mt CO₂ before the pressure limit was reached.

Figure 7 shows the results when the absolute permeability is multiplied by a factor of 2. The field pressure is not reaching the threshold pressure as the pressure can dissipate faster due to the higher absolute permeability. Due to a more favourable pressure communication the structure can potentially be filled to a larger extend still limited by the spill point.

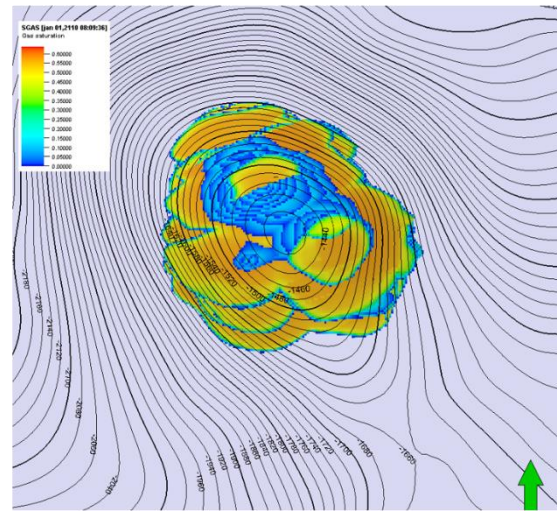
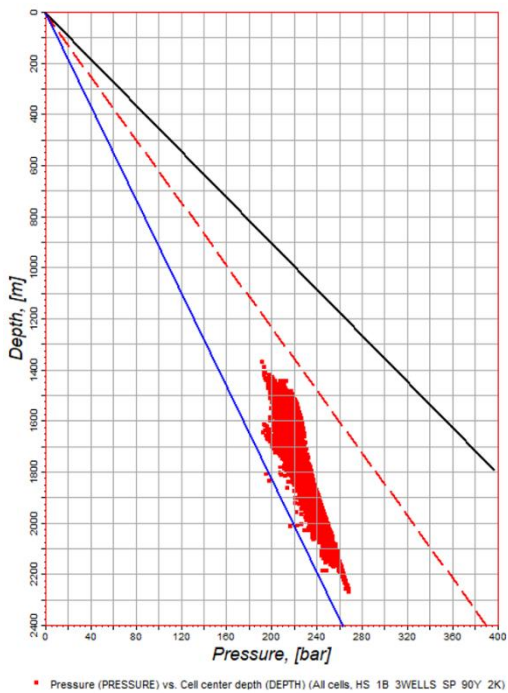


Figure 7. Left: Pressure versus depth diagram, blue line is the hydrostatic pressure, black line is the lithostatic pressure, red dotted line is the fracture threshold of 75% of the lithostatic pressure, red squares are the simulated grid cell pressure. Right: CO₂ distribution within the structural closure. The absolute permeability is increased by a factor of 2.

In figure 8 is shown the results, when the absolute permeability is decreased by a factor of 2. The formation water cannot be displaced as effective as for the previously cases and the pressure exceed the limiting pressure. The injection must be stopped before the structure is filled as effectively as the previous cases.

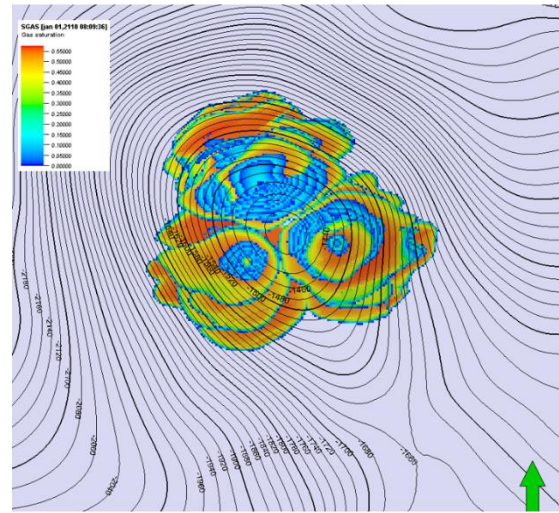
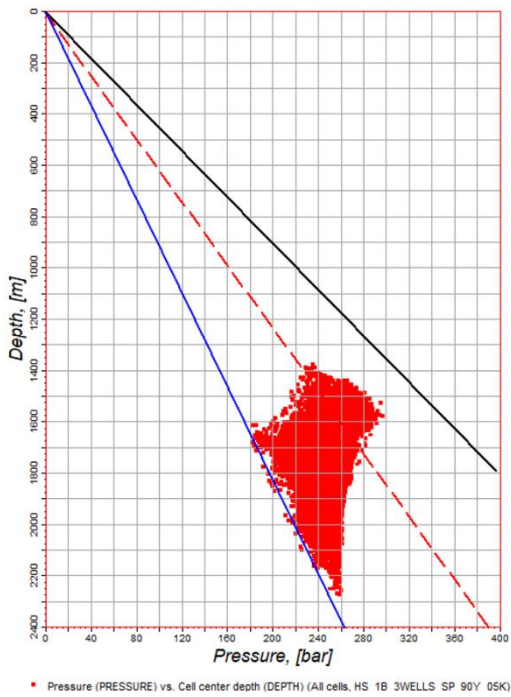


Figure 8. Left: Pressure versus depth diagram, blue line is the hydrostatic pressure, black line is the lithostatic pressure, red dotted line is the fracture threshold of 75% of the lithostatic pressure, red squares are the simulated grid cell pressure. Right: CO₂ distribution within the structural closure. The absolute permeability is decreased by a factor of 2.

If the relative permeabilities are changed instead of the absolute permeability the effect on the pressure distribution is insignificant compared to the base case, but the structure can contain more CO₂ due to the lower residual water saturation, cf. figure 9.

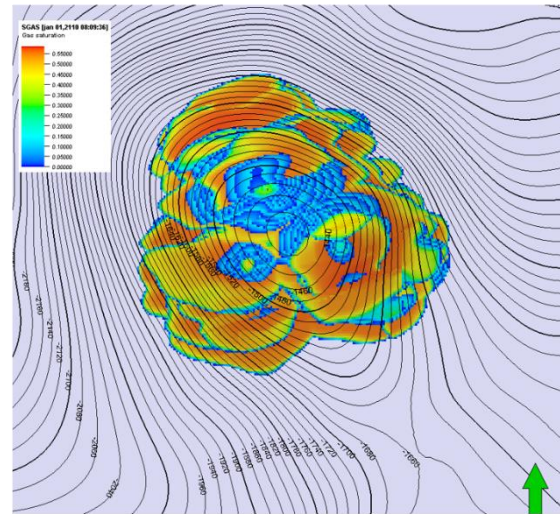
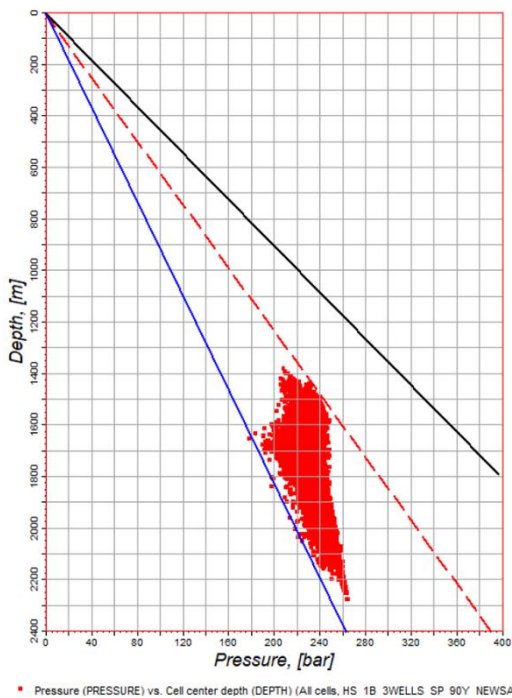


Figure 9. Left: Pressure versus depth diagram, blue line is the hydrostatic pressure, black line is the lithostatic pressure, red dotted line is the fracture threshold of 75% of the lithostatic pressure, red squares are the simulated grid cell pressure. Right: CO₂ distribution within the structural closure. The relative permeability to water has a lower residual water saturation compared to the base case.

When the N/G is shifted to a more favourable ratio of 0.9 compared to the base case of 0.5, the results for the pressure distribution are similar to the case with the higher permeability, *i.e.* the pressure can dissipate faster and will not increase to the limit. The total storage capacity will be higher compared to the base case.

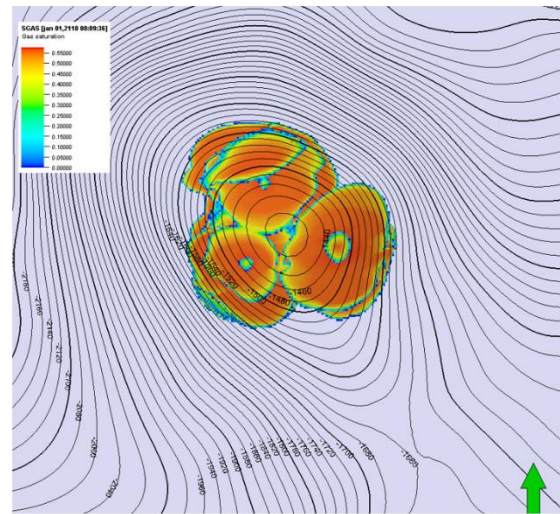
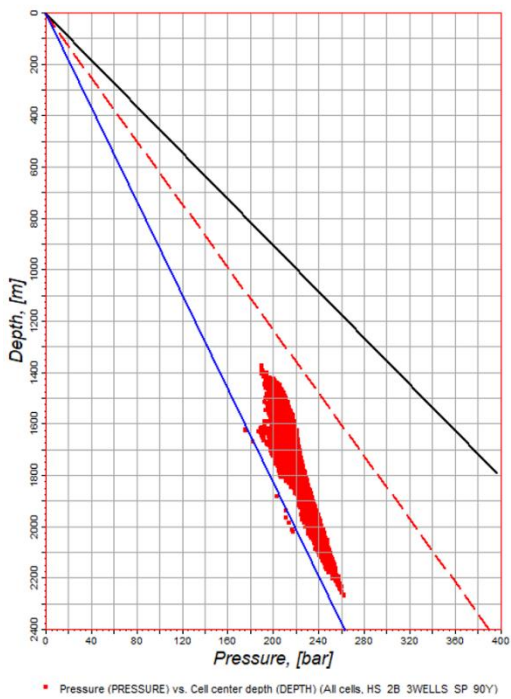


Figure 10. Left: Pressure versus depth diagram, blue line is the hydrostatic pressure, black line is the lithostatic pressure, red dotted line is the fracture threshold of 75% of the lithostatic pressure, red squares are the simulated grid cell pressure. Right: CO₂ distribution within the structural closure. N/G set to 0.9.

Figure 11 and 12 show the results for the case with a NWN trend in the depositional setting. Again, the pressure development for the case with a high N/G is less severe and more pore space available for storage, which is illustrated by the CO₂ plume is more concentrated around the injection points. Comparing figure 11 with 6, the effect from the orientation in depositional environments is shown to have only minor effect on the pressure and CO₂ distributions.

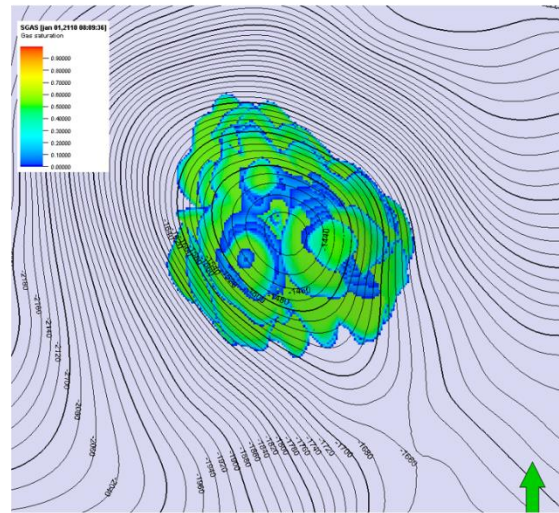
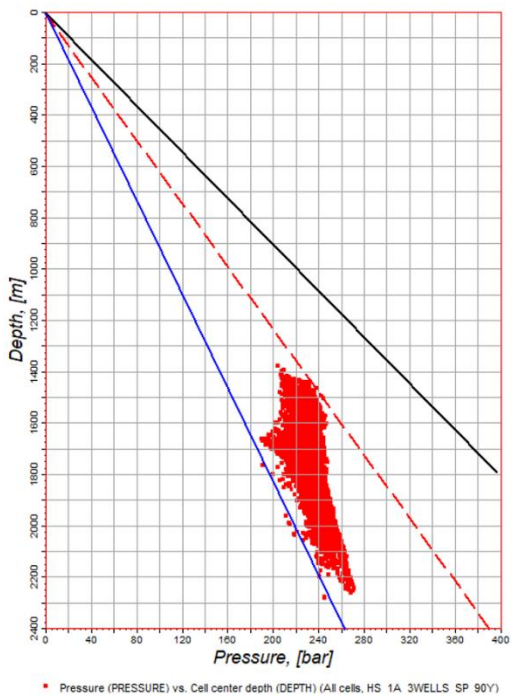


Figure 11. Left: Pressure versus depth diagram, blue line is the hydrostatic pressure, black line is the lithostatic pressure, red dotted line is the fracture threshold of 75% of the lithostatic pressure, red squares are the simulated grid cell pressure. Right: CO₂ distribution within the structural closure. NWN trend, N/G=0.5.

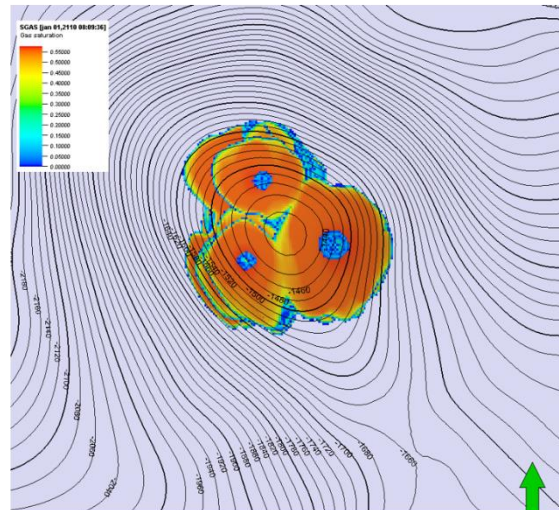
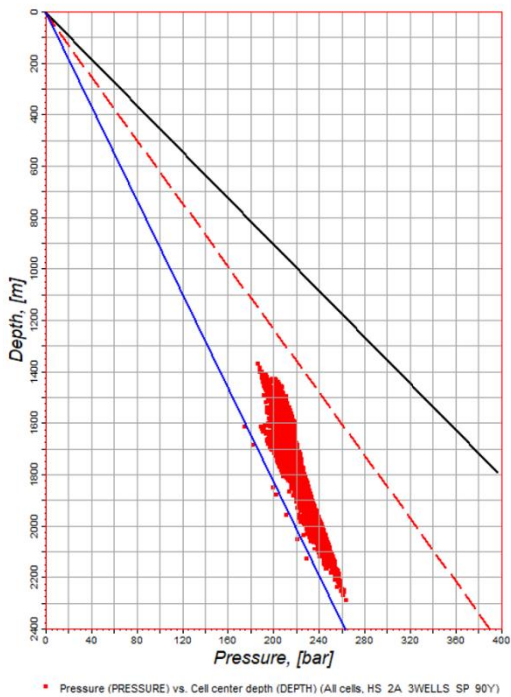


Figure 12. Left: Pressure versus depth diagram, blue line is the hydrostatic pressure, black line is the lithostatic pressure, red dotted line is the fracture threshold of 75% of the lithostatic pressure, red squares are the simulated grid cell pressure. Right: CO₂ distribution within the structural closure. NWN trend, N/G=0.9.

Conclusion

For the present modelling study, it was possible to optimize filling the structure without exceeding the pressure constraint. The simulation results show that pressure and CO₂ distributions are constrained by the interpretation and modelling of the depositional environment and the input reservoir properties.

The absolute permeability is the most constraining property, it has a direct impact on how fast the formation water can be displaced by the injected CO₂ and the pressure can dissipate. The same is seen with an increase in the N/G ratio, *i.e.* more high permeable sand relative to low permeable shale will dissipate pressure more effectively.

A high N/G ratio will leave more accessible pore space for the injected CO₂ and the plume will be more concentrated around the injection points resulting in a more efficient filling of the structure.

The present results are to be considered preliminary and mainly to be instructive for future work on modelling CO₂ injection in depositional settings.

A dynamic storage capacity for the Havnsø structure is modelled to be around 270 Mt of CO₂. It must be stressed that the number is dependent on the different assumptions and choices taken in the modelling procedure, both geological and operational. The number is comparable with the static capacity estimated in Hjelm *et al.* (2020) to be around 300 Mt. The static evaluation uses an efficiency factor of 0.4.

A simple simulation exercise with the Hanstholm model resulted in a dynamic storage capacity of 1000+ Mt. This is compared with the static estimated of 1340 Mt (Hjelm *et al.*, 2020).

Recommendations for future work

To de-risk any future decisions on development of full-scale CCS operations on the Havnsø and Hanstholm structures a series of essential studies are recommended. The simulation study shows that the principal constraining factor for an effective filling of the structures is the development in pressure.

The pressure development in the reservoir depends heavily on the absolute permeability operational constraints; well configurations (number and locations), injection rates and well completion intervals. Operational constraints will to a great extent be governed by demand for speed and economics for the individual storage operations.

- Determination of the absolute or effective permeability of the reservoir sandstone intervals in the Gassum Formation. GEUS' data base on core determined permeabilities are to be qualified with permeabilities determined from well tests. New and targeted well test are crucial in that respect.
- Intra shale layers influence on both the pressure development and the distribution of the injected CO₂. Information on the geological depositional processes/environment are essential to guide the distribution of the different layers/properties in the static (and Dynamic) model.
- Porosity, N/G, residual saturations and capillary properties of the intra-shale layers are decisive for the total storage capacity and must be evaluated.

References

- Batzle, M. and Wang, Z. 1992: Seismic properties of pore fluids, *Geophysics*, Vol. 57, No. 11, Nov. 1992, pp.1396-1408
- Bech, N. and Larsen, M., 2005: Storage of CO₂ in the Havnsø aquifer - a simulation study. A CO2STORE contribution. Danmarks og Grønlands Geologiske Undersøgelse Rapport 2005/9, 2001/89, 32 pp.
- Bennion, D.B. and Bachu, S. 2006(1): Supercritical CO₂ and H₂S – Brine Drainage and Imbibition Relative Permeability Relationships for Integral Sandstone and Carbonate Formations, Paper SPE 99325, SPE/DOE Symposium on Improved Oil Recovery, Tulsa, Oklahoma, 22 – 26 April. 2006.
- Bennion, D.B. and Bachu, S. 2006(2): Supercritical CO₂ and H₂S – Brine Drainage and Imbibition Relative Permeability Relationships for Integral Sandstone and Carbonate Formations, Paper SPE 99326, SPE Europec/Eage Annual Conference and Exhibition, Vienna, Austria, 12 – 15 June. 2006.
- Berg, S. and Ott, H. 2012. Stability of CO₂-brine immiscible displacement. *Int. J. Greenhouse Gas Control*, 11, 2012, pp. 188-203.
- Calsep A/S 2001: PVTsim-11.
- Chang, Yih-Bor, Coats, B.K. and Nolen, J.S. 1998: A Compositional Model for CO₂ Floods Including CO₂ Solubility in Water, *SPE RE&E*, April, 155-160.
- ECLIPSE 100., 2017. Schlumberger Information Solutions.
- Frykman, P. 2020a: Reservoir model for Hanstholm (Part of work package 6 in the CCUS project). Danmarks og Grønlands Geologiske Undersøgelse Rapport 2020/43.
- Frykman, P. 2020b: Reservoir model for Havnsø (Part of work package 6 in the CCUS project). Danmarks og Grønlands Geologiske Undersøgelse Rapport 2020/44.
- Hjelm, L., Anthonsen, K.L., Dideriksen, K., Nielsen, C.M., Nielsen, L.H. and Mathiesen, A. 2020. Evaluation of the CO₂ storage potential in Denmark (Part of work package 5 in the CCUS project). Danmarks og Grønlands Geologiske Undersøgelse Rapport 2020/46.
- Kristensen, L. 2020. Reservoir data – Stenlille area (Part of work package 6 in the CCUS project). Danmarks og Grønlands Geologiske Undersøgelse Rapport 2020/28.
- Peneloux, A., Rauzy, E. and Fréze, R.: A consistent correction for Redlich-Kwong-Soave volumes, *Fluid Phase Equilibria* **8**, 7-23, 1982.

Petrel. 2017. Schlumberger Information Solutions.

Rowe, A.M. and Chow, J. C. 1970: Pressure-Volume-Temperature-Concentration Relations of Aqueous NaCl Solutions, *J. of Chemical and Engineering Data*, Vol. 15, No. 1, 1970, pp.61-66.

Springer, N., Dideriksen, K., Holmslykke, H.D., Kjøller, C., Olivarius, M. and Schousbo, N. 2020. Seal capacity and geochemical modelling (Part of work package 5 in the CCUS project). Danmarks og Grønlands Geologiske Undersøgelse Rapport 2020/30.